Journal of Photochemistry & Photobiology, B: Biology 170 (2017) 140–151

Contents lists available at ScienceDirect

Journal of Photochemistry & Photobiology, B: Biology

journal homepage: www.elsevier.com/locate/jphotobiol

Phototoxic action of a zinc(II) phthalocyanine encapsulated into poloxamine polymeric micelles in 2D and 3D colon carcinoma cell cultures

Nicolás Chiarante[a], María C. García Vior[a], Josefina Awruch[b], Julieta Marino[a], Leonor P. Roguin[a,*]

[a] Universidad de Buenos Aires, Consejo Nacional de Investigaciones Científicas y Técnicas, Instituto de Química y Fisicoquímica Biológicas (IQUIFIB), Facultad de Farmacia y Bioquímica, Junín 956, C1113AAD Buenos Aires, Argentina

[b] Universidad de Buenos Aires, Facultad de Farmacia y Bioquímica, Departamento de Química Orgánica, Junín 956, C1113AAD Buenos Aires, Argentina

ARTICLE INFO

Keywords:
Photodynamic therapy
Phthalocyanine
Spheroid
Apoptosis
Murine colon carcinoma

ABSTRACT

Photodynamic therapy is emerging as a hopeful method for the treatment of oncological diseases. In the search of novel therapeutic strategies for colorectal cancer, in this work we reported the photocytotoxic activity of a lipophilic zinc(II) phthalocyanine on a murine colon adenocarcinoma cell line (CT26 cells). The 2,9(10),16(17),23(24) tetrakis[(2-dimethylamino)ethylsulfanyl]phthalocyaninatozinc(II), named Pc9, was encapsulated into Tetronic® 1107 polymeric poloxamine micelles (T1107) and assayed in 2D and 3D cell cultures. We showed that the formulation Pc9-T1107 was efficient to reduce cell viability after photodynamic treatment both in 2D cultures (IC_{50} 10 ± 2 nM) as well as in CT26 spheroids (IC_{50} 370 ± 11 nM). Cellular uptake of Pc9-T1107 was a time- and concentration-dependent process, being the phthalocyanine formulation mainly incorporated into lysosomal vesicles and endoplasmic reticulum cisterns, but not in mitochondria. Pc9-T1107 also induced the formation of reactive oxygen species immediately after cell irradiation. We also found that the phototoxic action of Pc9-T1107 was partially reversed in the presence of antioxidants, such as TROLOX and *N*-acetyl-cysteine. In addition, we showed that Pc9-T1107 treatment triggered an apoptotic cell death, as suggested by the detection of pyknotic nuclei, the reduction in the expression levels of procaspase-3 and the increase in caspase-3 enzymatic activity.

1. Introduction

Colorectal cancer (CRC) is the most common malignant disease of the gastrointestinal tract [1–3]. The incidence rate is higher in developed countries and many risk factors, including hereditary factors, obesity, diabetes, food habits or other lifestyle-related factors have been associated with its occurrence [1–6]. Nowadays, the CRC is the third most frequent cancer worldwide and the fourth cause of cancer death [2–5]. Although the introduction of new therapeutic agents has improved patient response rate [7], the finding of novel strategies with reduced toxicity and resistance still represents a challenge in the field of oncology.

Photodynamic therapy (PDT) is a selective and non-invasive method for the treatment of different types of cancer and other dermatological, cardiovascular and ophthalmic diseases [8–12]. Unlike conventional cancer treatments, this therapeutic approach represents an alternative that can be employed in a variety of endoscopically accessible tumors with a minimal damage to surrounding normal tissues [8,9,12–15]. PDT uses a nontoxic photosensitizer which upon irradiation with visible light produces reactive oxygen species (ROS) that lead to tumor cell destruction [8–16]. Phthalocyanines (Pcs) have been found to be optimal photosensitizers for PDT. Besides their well-known chemical stability, Pcs exhibit a high absorption coefficient in the visible region of the spectrum, mainly in the photo-therapeutic window (600–800 nm) where tissue light penetration is optimal, and are also efficient generators of singlet oxygen [10,16–20].

Targeted drug delivery systems are developed to reduce drug degradation, prevent harmful side effects, improve drug water solubilization and increase drug bioavailability. Many drug nanocarriers such as nanoparticles, lipoproteins, liposomes, nanoemulsions, dendrimers and amphiphilic polymers based micellar systems are extensively used [21–23]. Among the drug nanocarriers, polymeric micelles-based nanophotosensitizers show remarkable potential due to their large solubilization power, more loading capacity, high biocompatibility, enhanced photodynamic efficacy and higher stability in blood stream [24–26].

We have previously reported the cytotoxic potency of the lipophilic phthalocyanine Pc9 (2,9(10),16(17),23(24)-tetrakis-[(2-dimethylamino)ethylsulfanyl]phthalocyaninato zinc(II)) incorporated into nanocarriers, such as liposomes or polymeric micelles, in a human nasopharynx

* Corresponding author at: Instituto de Química y Fisicoquímica Biológicas (UBA-CONICET), Facultad de Farmacia y Bioquímica, Junín 956, C1113AAD Buenos Aires, Argentina.
E-mail address: rvroguin@qb.ffyb.uba.ar (L.P. Roguin).

http://dx.doi.org/10.1016/j.jphotobiol.2017.04.009
Received 13 January 2017; Received in revised form 14 March 2017; Accepted 10 April 2017
Available online 11 April 2017
1011-1344/

KB carcinoma cell line [27,28]. A higher phototoxic activity was showed after encapsulation of Pc9 into different poloxamine micelles (Tetronic®: T1107 or T1307) in comparison with either liposomes or the unencapsulated phthalocyanine [27,28]. Thus, taking into account that Pc9 loaded into micelles formulations behaved as a promising second-generation photosensitizer, we herein decided to examine the effectiveness of Pc9-T1107 in the murine colon carcinoma CT26 cell line. We showed that Pc9-T1107 exerted an effective phototoxic activity both in 2D and 3D cultures. In addition, we demonstrated that after localizing mainly in lysosome vesicles and endoplasmic reticulum cisterns, Pc9-T1107 induced an oxidative response mediated by the generation of reactive oxygen species (ROS), which finally led to some morphological and biochemical changes typical of an apoptotic cell death.

2. Materials and Methods

2.1. Chemicals

Synthesis and purification of the sulfur-linked 2,9(10),16(17),23(24) tetrakis[(2-dimethylamino)ethylsulfanyl]phthalocyaninatozinc(II), named Pc9 (Fig. 1A), has been previously described [17]. The probe 2′,7′-dichlorfluorescein diacetate, *N*-acetyl-L-cysteine, 6-hydroxy-2,5,7,8-tetramethylchroman-2-carboxylic acid (TROLOX), Höechst 33258 and propidium iodide were obtained from Sigma Chemical (St. Louis, MO). Polyclonal antibodies against actin and procaspase-3 were obtained from Santa Cruz Biotechnology (Santa Cruz, CA). MitoTracker Green FM, ER-Tracker Blue-White DPX and LysoTracker Green DND-26 were obtained from Invitrogen (Eugene, OR). Poloxamine Tetronic® 1107 (T1107, MW 15 kDa) was a gift from BASF (Germany) (Fig. 1B). Caspase substrate Ac-DEVD-AMC (caspase-3) was obtained from Peptide Institute Inc. (Osaka, Japan).

2.2. Cells and Culture Conditions

Murine colon carcinoma CT26 cells (ATCC CRL-2638) were maintained in RPMI-1640 (Gibco BRL) containing 10% (v/v) fetal bovine serum (FBS, Gibco BRL), 2 mM L-glutamine, 50 U/ml penicillin and 50 mg/ml streptomycin, in a humidified atmosphere of 5% CO_2 at 37 °C. Human colorectal adenocarcinoma SW480 (ATCC CCL-228), HT-29 (ATCC HTB-38) and Caco-2 cells (ATCC HTB-37) were grown in Dulbecco's modified Eagle Medium High Glucose (DMEM; Gibco BRL) supplemented with 10% (v/v) FBS, 2 mM L-glutamine, 50 U/ml penicillin, 50 mg/ml streptomycin and 1 mM sodium piruvate.

2.3. Photocytotoxicity in 2D Cultures

CT26, Caco-2, HT-29 and SW480 cells were plated at a density of 2×10^4 cells/well in 96-well microplates and incubated overnight at 37 °C until 70–80% of confluence. Then, the culture medium was replaced by medium containing 4% FBS and different concentrations of empty or Pc9-loaded T1107 micelles. After 24 h, compounds were

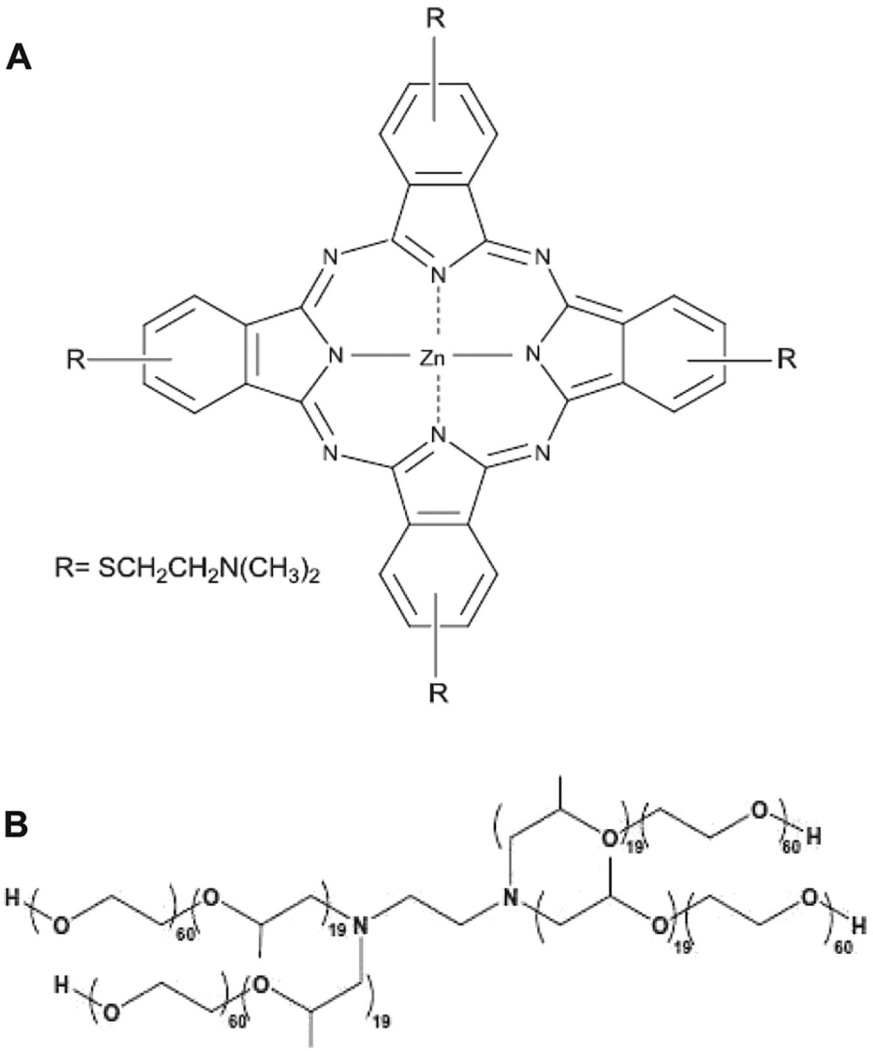

Fig. 1. Chemical structure of phthalocyanine 9 (A) and T1107 poloxamine micelles (B).

removed and cells were exposed to a light dose of 2.8 J cm^{-2}, 1.17 mW cm^{-2}, with a 150 W halogen lamp equipped with a 10 mm water filter to maintain cells cool and attenuate IR radiation. In addition, a cut-off filter was used to bar wavelengths shorter than 630 nm, as described previously [17]. In parallel, non-irradiated cells were used to study dark cytotoxicity. Following treatment, cells were incubated for an additional 24 h period and cell viability was determined by the MTT reduction assay. The absorbance (595 nm) was measured in a Biotrack II Microplate Reader (GE Healthcare, Piscataway, NY). The cytotoxic effect of 20 nM of Pc9-T1107 was also determined 24 h after irradiation at different light doses. Alternatively, cells treated with 20 nM of Pc9-T1107 were exposed to a light dose of 2.8 J cm^{-2} and cell survival was determined at different times after irradiation. In some experiments, cells were pre-incubated for 1 h before irradiation with different concentrations of antioxidants (TROLOX or *N*-acetyl-L-cysteine). After light exposure, cells were incubated for an additional 24 h period and cell number was evaluated by colorimetric determination of hexosaminidase levels as described previously [29].

2.4. Cellular Uptake and Outflow of Pc9

CT26 cells (1×10^6 cells/well) were grown overnight at 37 °C on 35 mm Petri dishes. Then, cells were incubated in culture medium containing 4% FBS with different concentrations of Pc9-loaded T1107 micelles for 24 h in the dark. After harvesting, cells were fixed 45 min with 1 ml of 70% cold ethanol and finally resuspended in 300 µl of phosphate-buffer saline (PBS). Drug cellular uptake was measured by determining the fluorescence emission of Pc9 with a BD Accuri C6 Plus cell cytometer at 640 nm excitation and 675 nm emission wavelengths. Cellular uptake was also determined after incubating cells from 30 min to 24 h in the dark with a 20 nM solution of Pc9-T1107.

CT26 cells (1.5×10^5 cells/well) grown on 6-well microplates were incubated in culture medium containing 4% FBS and 200 nM of Pc9-T1107 for 24 h. Then, the medium was replaced by RPMI-1640 containing 10% FBS and cells were incubated for different time-periods. After harvesting, cells were lysed with 250 µl of dimethylformamide, and Pc9 fluorescence, corresponding to the amount of photosensitizer remaining in the cells, was monitored with a Jasco FP-6500 spectrofluorometer equipped with a Peltier thermostat at 691 nm excitation and 695–750 nm emission wavelengths. In order to minimize inner filter effects, all measurements were done in a 3-mm-pathlength quartz cell. Emission and excitation slits were set at 3 nm bandwidth.

2.5. Intracellular Localization of Pc9

CT26 cells grown on coverslips were incubated with 100 nM of Pc9 incorporated into T1107 micelle for 24 h at 37 °C in the dark. After washing with PBS, cells were stained with LysoTracker Green DND-26 (75 nM, 30 min), MitoTracker Green FM (100 nM, 45 min) or ER-Tracker Blue-White DPX (400 nM, 30 min), as described previously [27,28]. Cells were fixed for 10 min at room temperature with 4% paraformaldehyde and then examined by fluorescence with a confocal microscope Olympus FV 300. Pc9 was excited at 635 nm and the emission was monitored at wavelengths between 655 and 755 nm. Lysosomes and mitochondria were excited at 473 nm and green fluorescence was detected at 485–545 nm while endoplasmic reticulum were excited at 405 nm and blue fluorescence was detected at 425–460 nm. Cell nuclei were stained with Höechst 33258, excited at 405 nm and detected at 425–460 nm.

2.6. Determination of Intracellular Reactive Oxygen Species (ROS) Production

The endogenous ROS content was evaluated from the oxidation of the probe 2′,7′-dichlorfluorescein diacetate (DCFH-DA; Sigma Chemical, St. Louis, MO). After diffusing into cells, DCFH-DA is first deacetylated by esterases and then is oxidized by hydrogen peroxide or peroxides to produce the fluorescent 2′,7′-dichlorfluorescein (DCF). CT26 cells were plated at a density of 3×10^4 cells/well in 24-well microplates and incubated 48 h at 37 °C until 70–80% of confluence. Then, the culture medium was replaced by RPMI containing 4% FBS and different concentrations of Pc9-T1107. After 24 h, cells were washed with PBS and incubated 30 min at 37 °C in the presence of 10 µM DCFH-DA. After removing the probe, cells were irradiated with a light dose of 2.8 J cm^{-2} in the presence of RPMI containing 10% FBS. Cells were next solubilized by treating with Triton X-100 (0.1% v/v) in PBS for 30 min, and the green fluorescence of DCF was detected in a PerkinElmer LS55 Fluorometer (PerkinElmer Ltd., Beaconsfield, UK) using 488 nm excitation and 530 nm emission wavelengths. After 10 min of incubation with a final concentration of 50 µM propidium iodide (PI), DNA content was estimated from the fluorescence intensity of DNA-PI complex at excitation and emission wavelengths of 538 and 590 nm, respectively. Results were expressed as the ratio between DCF and PI fluorescence. Alternatively, ROS production was examined using a fluorescence Olympus BX50 microscope and quantified with the Image J software.

2.7. Formation of 3D Tumor Spheroids and Photocytotoxicity Study

The liquid overlay technique was used to generate spheroids [30]. Briefly, CT26 cells were plated at a density of 2×10^4 cells/well in U-shaped 96-well microplates pre-coated with 200 µl of 1% agarose. The formation of spheroids was checked by optical microscopy. Spheroids' size (volume) was examined by digital photography and analyzed using the Image J software. The average diameter of each spheroid was employed to estimate spheroid volume as $V = 4/3 \times \pi \times (d/2)^3$. In order to evaluate Pc9-T1107 cytotoxicity, five spheroids/well, formed after 72 h of seeding, were transferred into 24-well microplates containing culture medium with 4% FBS and different concentrations of Pc9-loaded T1107 micelles. After 24 h, compounds were removed and cells were exposed to a light dose of 2.8 J cm^{-2}. In parallel, non-irradiated spheroids were used to study dark cytotoxicity. After an additional 24 h period, cell viability was determined by the MTT reduction assay.

2.8. Nuclear Damage

CT26 cells were grown for 24 h on coverslips in the absence (control) or presence of different concentrations of Pc9-T1107. Immediately after irradiation, cells were washed twice with PBS and coverslips were fixed for 10 min at room temperature with 4% paraformaldehyde. After washing, Höechst 33258 (2 µg/ml) was employed to stain nuclei. Images were collected with a confocal microscope Olympus FV 300 (excitation at 405 nm and detection at 425–460 nm).

When CT26 spheroids were employed, cells were incubated in culture medium containing 4% FBS and 740 nM Pc9-T1107. After 24 h, cells were washed, irradiated, incubated for an additional 24 h, fixed and finally stained with Höechst 33258 (2 µg/ml) for 1 h at 37 °C. Nuclei were visualized with the confocal microscope Olympus FV 300.

2.9. Western Blot Assays

CT26 cells were incubated during 24 h with a 20 nM solution of Pc9-T1107, then washed with PBS and exposed to a light dose of 2.8 J cm^{-2}. After irradiation, suspensions containing 1×10^6 cells were immediately lysed for 30 min at 4 °C in 10 µl of lysis buffer (0.5% Triton X-100, 1 µg/ml aprotinin, 1 µg/ml trypsin inhibitor, 1 µg/ml leupeptin, 10 mM $Na_4P_2O_7$, 10 mM NaF, 1 mM Na_3VO_4, 1 mM EDTA, 1 mM PMSF, 150 mM NaCl, 50 mM Tris, pH 7.4). Alternatively, irradiated cells were incubated for different time-periods

at 37 °C and then cell lysates were prepared. Clear supernatants were obtained after centrifugation at 17,000 × *g* for 10 min at 4 °C and protein concentration was determined using Bradford reagent. When CT26 spheroids were employed, cells were incubated in culture medium containing 4% FBS and 2 × IC_{50} concentration of Pc9-T1107. After 24 h, cells were washed, irradiated, incubated for an additional 18–24 h and then washed again. Spheroids were incubated for 10 min in 0.25% trypsin-PBS at 37 °C and afterwards disintegrated using a pipette. Immediately, culture medium containing 10% FBS was added. Aliquots containing 50 μg of protein were resuspended in 0.063 M Tris/HCl, pH 6.8, 2% SDS, 10% glycerol, 0.05% bromophenol blue, 5% 2-ME, submitted to SDS-PAGE and then transferred onto nitrocellulose membranes (GE Healthcare, Piscataway, NY) for 1 h at 100 V in 25 mM Tris, 195 mM glycine, 20% methanol, pH 8.2. After blocking with 10 mM Tris, 130 mM NaCl and 0.05% Tween 20, pH 7.4, containing 3% bovine serum albumin (BSA), membranes were treated as the usual western blotting method. Immunoreactive proteins were visualized using the ECL detection system (Amersham Biosciences, Piscataway, NY) according to the manufacturer's instructions. For quantification of band intensity, Western blots were scanned using a densitometer (Gel Pro Analyzer 4.0). Equal protein loading was confirmed by reprobing membranes with a rabbit anti-actin antibody (Sigma-Aldrich, Inc., Missouri, USA).

2.10. Caspase Activity Assay

After incubating CT26 cells for 24 h with a 20 nM solution of Pc9-T1107, cells were washed and then irradiated with a light dose of 2.8 J cm^{-2} as previously described. Cells were then incubated for different time-periods at 37 °C and 1 × 10^7 cells were lysed for 30 min at 4 °C in 50 μl of lysis buffer (10 mM HEPES, pH 7.4, 50 mM NaCl, 2 mM $MgCl_2$, 5 mM EGTA, 1 mM PMSF, 2 μg/ml leupeptin, 2 μg/ml aprotinin) followed by three cycles of rapid freezing and thawing. Cell lysates were centrifuged at 17,000 × *g* for 15 min and total protein concentration was determined using Bradford reagent. Aliquots containing 100 μg of protein were diluted in assay buffer (20 mM HEPES, 132 mM NaCl, 6 mM KCl, 1 mM $MgSO_4$, 1.2 mM K_2HPO_4, pH 7.4, 20% glycerol, 5 mM DTT), and incubated at 37 °C for 1 h with 50 μM of the fluorogenic substrate for caspase-3 (Ac-DEVD-AMC). Cleavage of the substrate was monitored by AMC release in a SFM25 Konton Fluorometer at 355 nm excitation and 460 nm emission wavelengths.

2.11. Statistical Analysis

The values are expressed as mean ± S.E.M. Statistical analysis of the data was performed by using the Student's *t*-test or one way analysis of variance (ANOVA) followed by Dunnett post-hoc test where appropriate. $p < 0.05$ denotes a statistically significant difference.

3. Results

3.1. Photocytotoxicity in 2D Cultures

In order to examine the cytotoxic action of Pc9 loaded into T1107 micelles on different colon carcinoma cell lines (CT26, Caco-2, HT-29, SW480), we first evaluated the effect of empty micelles on cell survival by using the MTT assay. As shown in Fig. 2A for CT26 cells, the micellar formulation did not affect cell survival either in the dark or in the presence of a light dose of 2.8 J cm^{-2}, indicating that T1107 did not show a cytotoxic effect up to a 0.5% concentration. Similar results were obtained on the other tumor cell lines (data not shown). On the other hand, a cytotoxic effect was effectively observed after irradiation of Pc9-T1107-loaded CT26 cells, being the 50% inhibition of cell proliferation (IC_{50} value) achieved at a concentration of 10 ± 2 nM (Fig. 2B, Table 1). A comparable pattern of reactivity was found on the other cancer cell lines (Table 1). Further studies were then performed with CT26 cells. The photocytotoxicity of a 20 nM concentration of Pc9-T1107 on CT26 cells was next evaluated at different light doses. A light dose-dependent decrease of cell viability was shown, reaching the maximum effect at a PDT light dose of 2.8 J cm^{-2} (Fig. 2C).

Since the cytotoxic action of Pc9-T1107 was initially determined 24 h post-irradiation (p.i.), we further examined cell survival kinetics at shorter times after irradiation. As shown in Fig. 2D, when cells were incubated with 20 nM of Pc9-T1107, cell viability decreased and declined gradually from 3 to 24 h p.i. A reduction in the number of cells together with a change in cell morphology was evident after visualizing cells by phase contrast microscopy (Fig. 2E).

3.2. Uptake, Outflow and Intracellular Localization of Pc9-T1107 in CT26 Cells

The cellular uptake of a 20 nM concentration of Pc9 incorporated into T1107 micelles was determined after incubating CT26 cells in the dark for different times (Fig. 3A). A significant uptake was detected after 30 min of treatment, and a constant intracellular concentration was reached after 6 h of incubation and maintained for at least 24 h. In addition, it was demonstrated that Pc9-T1107 was incorporated into CT26 cells in a lineal concentration-dependent manner, suggesting that the uptake is a non-saturable process up to a 100 nM Pc9 concentration (Fig. 3B). The kinetics of Pc9 outflow was also studied after incubating Pc9-loaded CT26 cells in culture medium free of photosensitizer. A significant decrease in the intracellular amount of Pc9 was observed after 3 h of incubation, declining this amount gradually up to 48 h, the maximal tested time (Fig. 3C).

The intracellular localization of Pc9-T1107 was further studied by confocal microscopy. As shown in Fig. 3D, the typical red fluorescence emission of Pc9 was mostly observed in the cytosol after incubating CT26 cells for 24 h in the dark. No nuclear Pc9 entrance was evident, as suggested by the lack of overlay of the red fluorescence of Pc9 and the Höechst 33258 nuclear signal (Fig. 3D). The subcellular localization of Pc9-T1107 was further studied after incubating CT26 cells for 24 h in the dark and staining them with fluorescent dyes for specific organelles, such as LysoTracker Green for lysosome, ER-Tracker Blue-White for endoplasmic reticulum, and MitoTracker Green for mitochondria. Images obtained by confocal microscopy showed that the red fluorescence of Pc9 co-localized with the green fluorescence of the specific lysosome probe (yellow vesicles) and the blue fluorescence of the ER probe (violet vesicles) (Fig. 4). No overlapping was observed between the red signal of Pc9 and the green fluorescence of the mitochondria probe, indicating that Pc9 did not localize in this organelle (Fig. 4).

3.3. Intracellular Production of ROS in Pc9-T1107 Treated-cells

We have previously studied the photodynamic properties of Pc9 encapsulated into different micelles, including T1107, and demonstrated that all Pc9-loaded micellar formulations were capable of generating singlet molecular oxygen [28]. In this study, we decided to examine the formation of ROS after irradiation of CT26 cells pretreated with different concentrations of Pc9-T1107. Quantitative evaluation of ROS levels was performed immediately after cell irradiation with the probe DCFH-DA, which is oxidized to the green fluorescent DCF in the presence of ROS. Results showed in Fig. 5A revealed that ROS levels significantly increased from a 10 nM Pc9-T1107 concentration, which represents the IC_{50} value, up to a 50 nM concentration. A concentration-dependent increase in the green DCF fluorescence was also observed by fluorescence microscopy of irradiated cells treated with Pc9-T1107 (Fig. 5B).

The effect of different concentrations of two antioxidants, TROLOX and *N*-acetyl-cysteine (NAC), on the antiproliferative action induced by Pc9-T1107 was further explored. Both antioxidants partially reversed the inhibitory effect of Pc9 on cell survival, suggesting that ROS are mediating Pc9-triggered cell death (Fig. 6A and B). While NAC did not

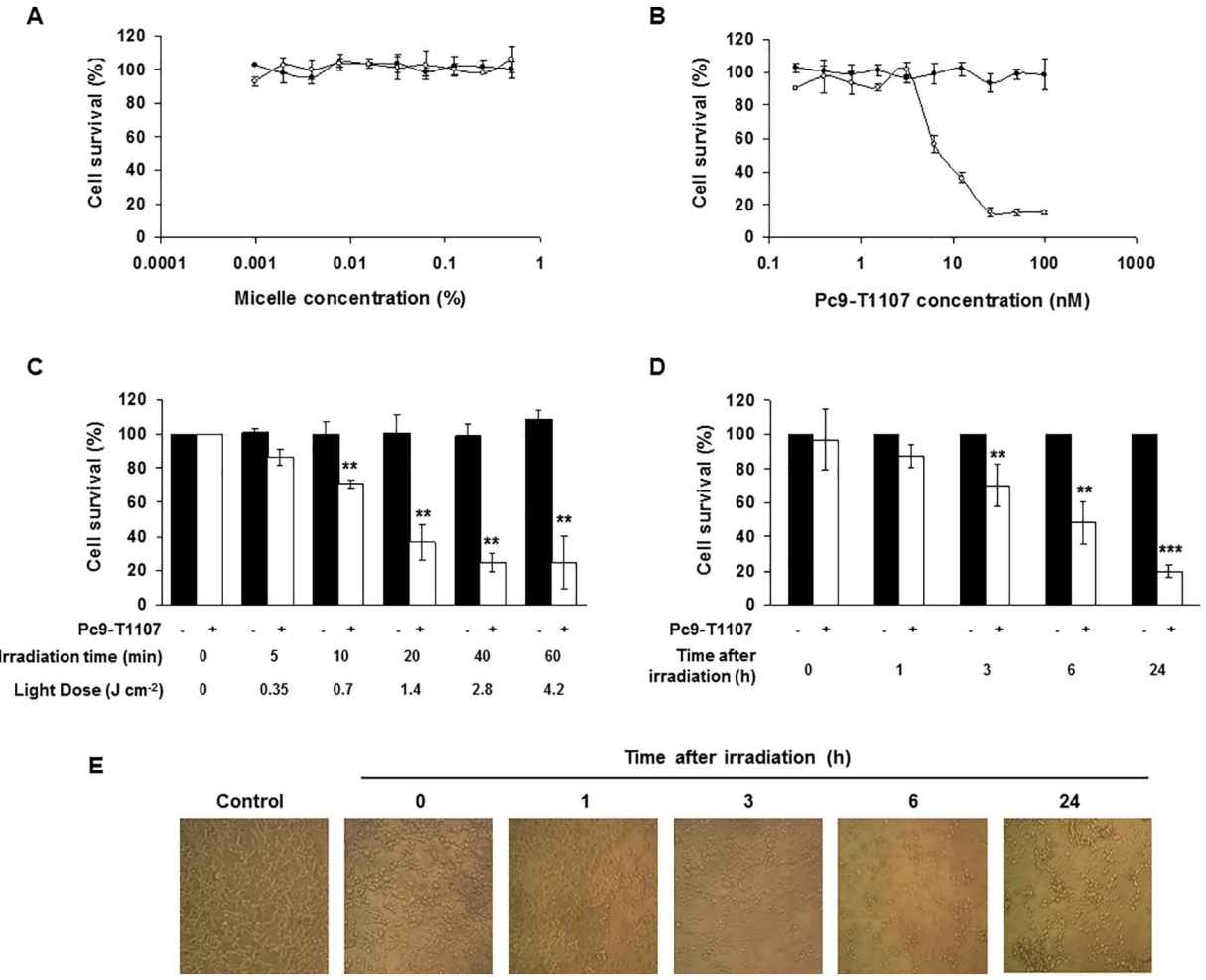

Fig. 2. Effect of T1107 and Pc9-T1107 on CT26 cell viability. Different concentrations of T1107 micelle (A) or Pc9-T1107 (B) were incubated with CT26 cells in the dark (●) or exposed to a light dose of 2.8 J cm^{-2} (○). CT26 cells were incubated with or without Pc9-T1107 (20 nM) and exposed to different PDT light doses (C) or to a light dose of 2.8 J cm^{-2} (D). The MTT assay was carried out after 24 h (C) or at different times after irradiation (D) as described under Materials and Methods. Results are expressed as the percentage of cell survival with respect to that obtained in the absence of Pc9-T1107 (control) and represent the mean ± S.E.M. of five different experiments. $^{**}p < 0.005$, $^{***}p < 0.0001$, significantly different from non-irradiated cells. (E) Phase contrast images of CT26 cells at different times post irradiation. Magnification: 100 ×.

Table 1
Photocytoxicity of Pc9-T1107 in colon carcinoma cell lines.

Cell line	IC_{50} (nM)[a]
CT26	10 ± 2
Caco-2	11 ± 1
HT-29	6 ± 1
SW480	6 ± 1

[a] The molar drug concentrations required to cause 50% growth inhibition (IC_{50}) were determined from dose-response curves. Results represent the mean ± S.E.M. of at least three different experiments.

show a cytotoxic effect on cells incubated in the absence of Pc9-T1107, a reduction in cell survival was determined for unloaded cells exposed to 10 mM TROLOX. The protective effect of 5 mM TROLOX, a non-toxic concentration, was also evident by phase contrast microscopy (Fig. 6C).

3.4. Photocytotoxicity in 3D Cultures

Since spheroids are a suitable *in vitro* model to approach the knowledge of the *in vivo* behavior of drugs [30,31], the cytotoxic effect of Pc9 micellar formulation was also determined in 3D cultures. When different concentrations of Pc9-T1107 were incubated with CT26 spheroids, no effect on cell survival was evident in the dark, while a significant decrease was shown after irradiation, being the IC_{50} value of 370 ± 11 nM (Fig. 7A). As a result, after incubating spheroids for different periods of time, the volume of Pc9-treated spheroids was smaller than non-treated spheroids (Fig. 7B). Furthermore, spheroid growth kinetics was dependent on Pc9 concentration. Thus, a more pronounced Pc9 growth inhibitory effect was obtained with 5 × IC_{50} of Pc9 (Fig. 7B and C).

3.5. Pc9-T1107 Induced an Apoptotic Cell Death

In order to examine the mechanism of cell death induced by Pc9-T1107, 2D CT26 cultures exposed to different concentrations of photosensitizer were stained with Höechst 33258 and visualized with a confocal microscope. As shown in Fig. 8A, highly condensed nuclei characteristic of apoptotic cells were observed at IC_{50} or 2 × IC_{50} of Pc9-T1107. For 3D CT26 spheroids, the presence of nuclei with chromatin condensation was more evident at 2 × IC_{50} of Pc9-T1107 (Fig. 8B). We further examined the involvement of the executioner caspase-3 in the apoptotic response induced by Pc9-T1107. A significant decrease in the expression levels of procaspase-3 was detected immediately after irradiation of CT26 cells preloaded with 2 × IC_{50} of Pc9-T1107 (20 nM), suggesting the activation by cleavage of the inactive procaspase (Fig. 8C). A reduction of procaspase-3 levels was

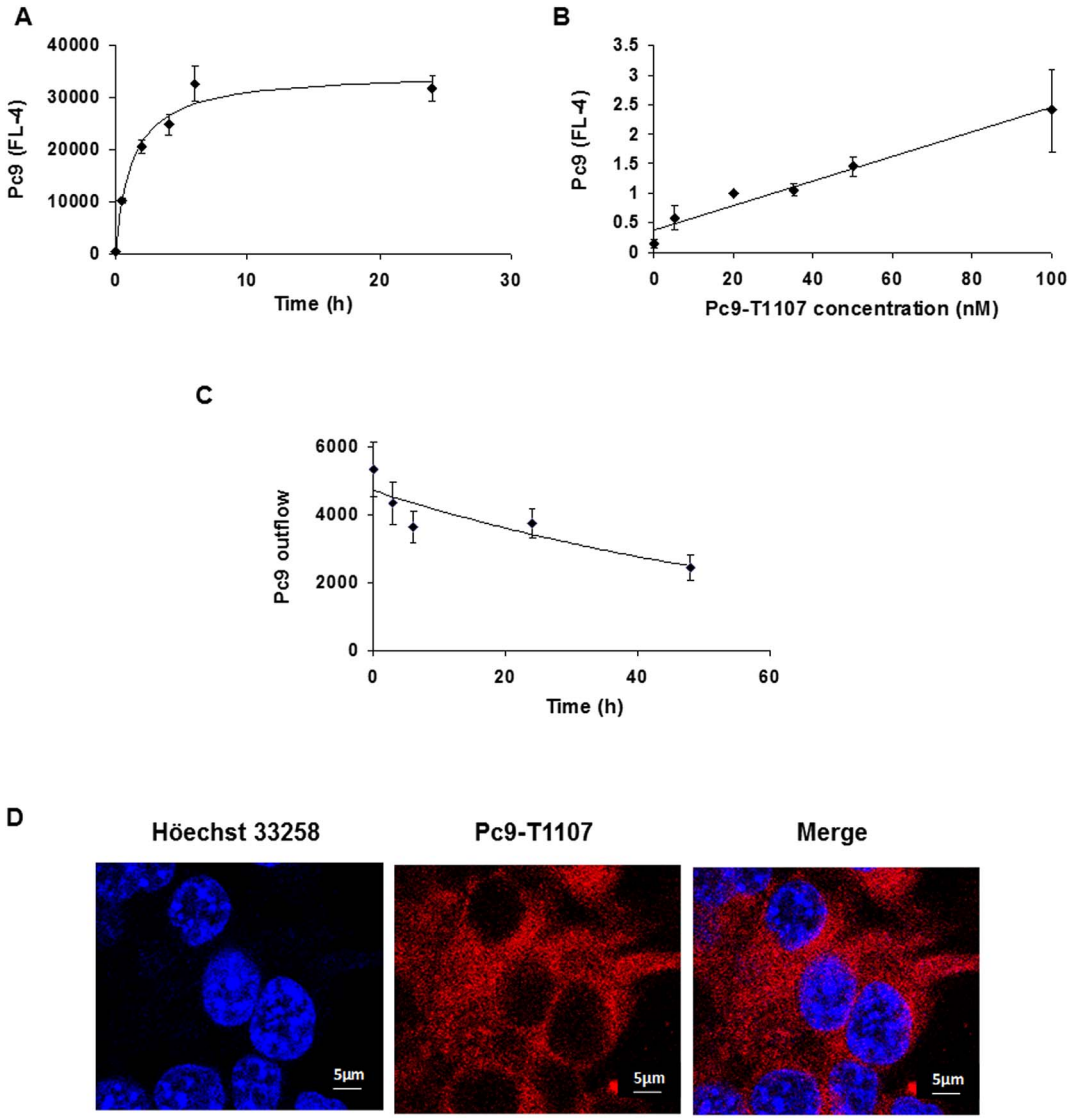

Fig. 3. Cellular uptake and outflow of Pc9-T1107. CT26 cells were incubated in the dark either with a 20 nM concentration of Pc9-T1107 for different time-periods (A) or with different Pc9-T1107 concentrations for 24 h (B). The uptake of Pc9 was determined by using a BD Accuri C6 Plus cell cytometer. (C) CT26 cells were incubated in the dark with Pc9-T1107 200 nM for 24 h and then incubated with culture medium for different time-periods. The outflow of Pc9 was determined by using a Jasco FP-6500 spectrofluorometer. (D) Intracellular localization of Pc9 was visualized by confocal microscopy after incubating CT26 cells for 24 h in the dark. Scale bar 5 µm. (For interpretation of the references to color in this figure, the reader is referred to the web version of this article.)

also shown 18 h and 24 h after light exposure of CT26 spheroids treated with 2× IC_{50} of Pc9-T1107 (740 nM) (Fig. 8D). The activation of caspase-3 in 2D CT26 cultures was also confirmed with a fluorescent activity assay. A slight increase in caspase-3 proteolytic activity seems to be detected at 1 h p.i., but significant increments were certainly obtained at 3 h and 24 h p.i. (Fig. 8E).

4. Discussion

PDT is a selective and non-invasive procedure that should be considered as an alternative strategy for cancer treatment [8,12,32]. In particular, the use of PDT in patients with CRC seems to be a safe and promising therapeutic modality. In this sense, several clinical trials with positive results employed PDT in the treatment of both precancerous conditions as well as advanced stages [33]. These clinical studies mainly evaluated the efficacy of various photosensitizers, such as 5-aminolevulinic acid and hematoporphyrin or chlorine derivatives for the treatment of CRC patients [33–35]. The phthalocyanines (Pcs) arose as a second-generation of photosensitisers which are activated at wavelengths around 670 nm, a region where light penetration into tissues is optimal [20,36]. The clinical response of some aluminium and silicon phthalocyanines has been assessed in phase I/II studies applied to the treatment of lung, esophageal and cutaneous malignancies [37,38], but no clinical trial has evaluated the photodynamic efficiency of phthalocyanines as photosensitizers in the treatment of patients with CRC [39]. In this work, the potential of a lipophilic phthalocyanine (Pc9) encapsulated into T1107 polymeric micelles was evaluated in colon carcinoma cells. Since the poor solubility of Pc9 under physiological conditions correlates with a low bioavailability and a decrease in the photodynamic efficiency, polymeric micelles were employed as proper nanocarriers to prevent the aggregation of Pc9. These micelles have nanosize (10–100 nm) and spherical supramolecular core/shell structures formed by self-assembly of amphiphilic copolymers at physiological conditions. The nanoscale polymer assemblies of the poloxamine micelle T1107 can incorporate the water-insoluble Pc9 in their hydrophobic core, protect them against chemical or biological degradation and avoid the reticuloendothelial system's uptake [40]. Moreover, polymeric micelles display several advantages over other excipients currently used in parenteral formulation in clinical practices for anticancer drugs such as dimethylsulfoxide, ethanol, polysorbate 80

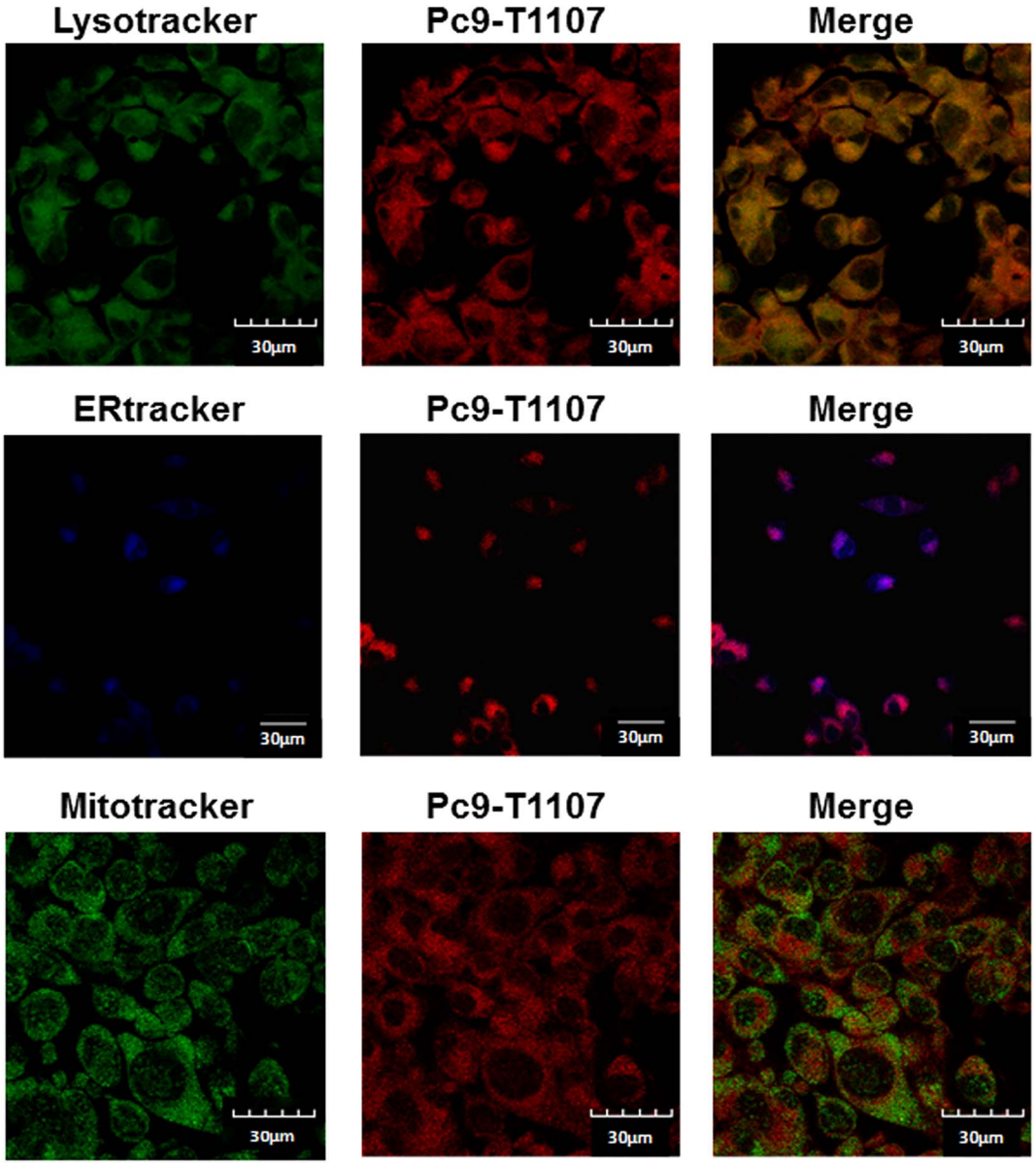

Fig. 4. Intracellular localization of Pc9-T1107. CT26 cells incubated for 24 h with 100 nM of Pc9-T1107 were stained with LysoTracker Green DND-26 (75 nM, 30 min), ER-Tracker Blue-White DPX (1000 nM, 30 min) or MitoTracker Green FM (100 nM, 45 min) as indicated in Materials and Methods. Red fluorescence corresponds to Pc9-T1107, green fluorescence represents the signal for lysosomes or mitochondrias, and blue fluorescence represents the ER signal. Scale bar 30 µm. (For interpretation of the references to color in this figure legend, the reader is referred to the web version of this article.)

(Tween 80®) and polyethoxylated castor oil (Cremophor EL®). They are safer for intravenous administration, they are more physically stable under dilution and they improve the bioavailability because they solubilize drugs more effectively [41].

The efficiency of the Pc9 formulation as a photocytotoxic agent was demonstrated not only in a conventional 2D culture model (IC_{50} 10 ± 2 nM), but also in 3D cultures of colon malignant cells (IC_{50} 370 ± 11 nM). In addition, we found a concentration-dependent growth reduction of Pc9-treated spheroids at different days after treatment. In accordance with other reports, the photosensitizer cytotoxic effect appeared to be less potent in 3D than in 2D cultures, a result that could be explained by some features of the spheroids resembling more an *in vivo* tumor, including the existence of a gradient of nutrient and oxygen, and the different light doses and photosensitizer concentration at the core or the edge of the spheroid [42–45].

We showed that Pc9 incorporated into T1107 micelles displayed some features required for a suitable photosensitizer [8,10–12,46]. Thus, Pc9 exerted a potent photocytotoxic effect on different colon carcinoma cell lines, without affecting cell survival in the dark. In addition, Pc9-T1107 induced the formation of reactive oxygen species upon CT26 cell irradiation. As it has been reported for other photosensitizers, these cytotoxic species are indeed mediating the oxidative damage that finally leads to cell death [8,47–49]. In this regard, the significant reversion of the growth inhibitory activity induced by Pc9-T1107 in the presence of antioxidants, such as TROLOX and NAC, indicated that ROS are certainly involved in CT26 death.

After studying the intracellular localization, we found that Pc9-T1107 mainly targeted lysosomes and endoplasmic reticulum. Based on the short lifetime and the short radius of diffusion of singlet oxygen, both lysosomes and endoplasmic reticulum would represent the primary sites that initiate the cascade of molecular events that finally lead to cell photodamage [50,51]. Although the intracellular location may vary according to the photosensitizer and the cell line studied, mitochondrial and/or lysosomal localization has been reported for chlorine, diarylporphyrin and 5-ALA derivatives evaluated *in vitro* in different colon carcinoma cells [52–54]. Based on our results, further

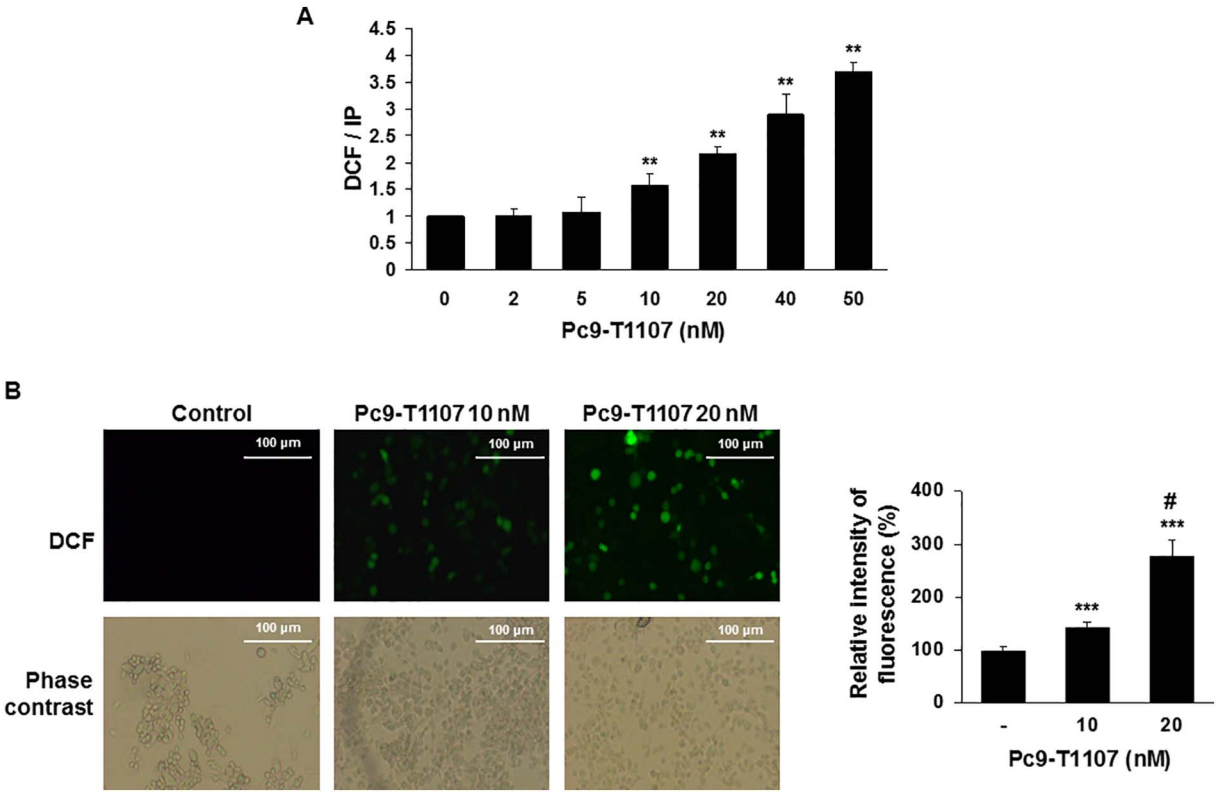

Fig. 5. Effect of Pc9-T1107 on ROS formation. (A) ROS levels were quantified with a fluorometer immediately after irradiation of Pc9-T1107-loaded CT26 cells as described in Materials and Methods. DNA content was estimated after incubating with PI and results are expressed as the ratio between DCF and PI fluorescence (mean ± S.E.M., n = 3, $^{**}p < 0.005$). (B) Alternatively, ROS formation was detected in CT26 cells plated on coverslips with a fluorescence microscope (upper panel). Cell morphology was examined by phase contrast microscopy (lower panel). Relative intensity of fluorescence was determined with the Image J software; results represent the mean ± S.E.M., n = 3, $^{***}p < 0.0001$, significantly different from cells incubated in the absence of Pc9-T1107; $^{\#}p < 0.0001$, significantly different from cells incubated with 10 nM Pc9-T1107. Scale bar 100 µm.

studies will be required to investigate the role played by lysosomes and endoplasmic reticulum in the photocytotoxic action induced by Pc9-T1107 in CT26 cells.

We also found some evidence of the cell death modality induced by Pc9-T1107 in CT26 cells. Thus, after PDT treatment, we observed the presence of both morphological and biochemical characteristics that support the induction of an apoptotic cell response. In particular, the decrease in the expression levels of procaspase-3 detected both in 2D as

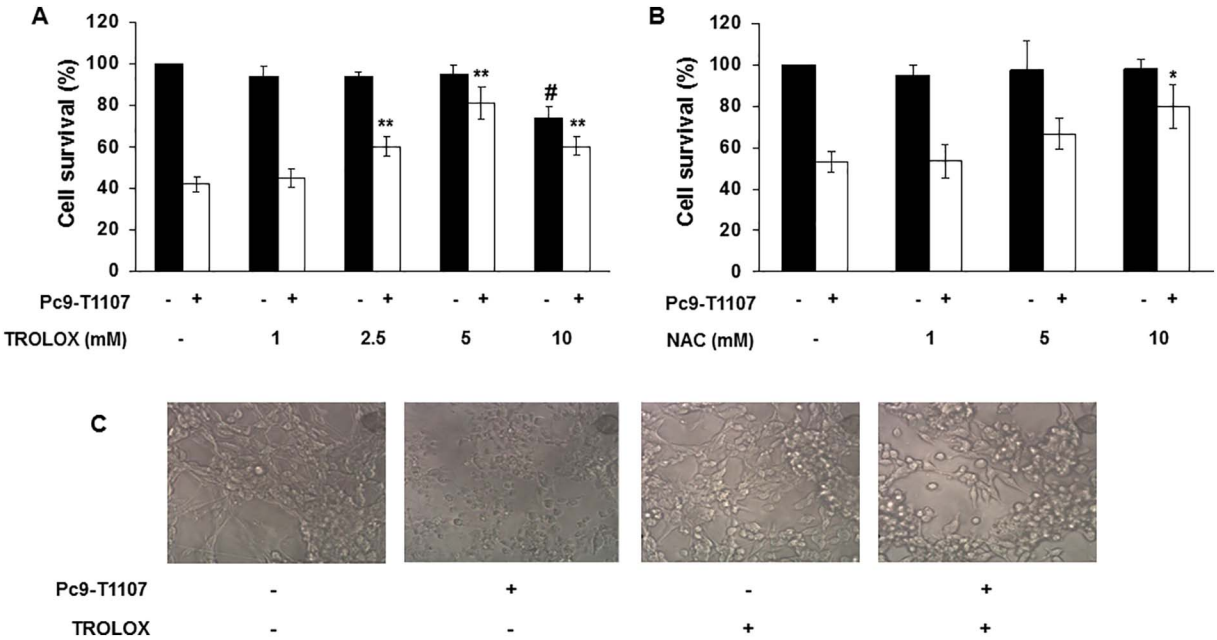

Fig. 6. Effect of antioxidants on PDT-induced cell death. After photodynamic treatment with a 10 nM concentration of Pc9-T1107, cell growth was determined in the absence or presence of different concentrations of TROLOX (A) or NAC (B) by the hexosaminidase method [29]. Results represent the mean ± S.E.M., n = 3, $^{*}p < 0.05$, $^{**}p < 0.005$, significantly different from cells treated with Pc9-T1107 in the absence of antioxidants; $^{\#}p < 0.0001$ significantly different from control (absence of Pc9-T1107). (C) Morphology of CT26 cells loaded or not with Pc9-T1107 and incubated with or without 5 mM TROLOX. Magnification: 200 ×.

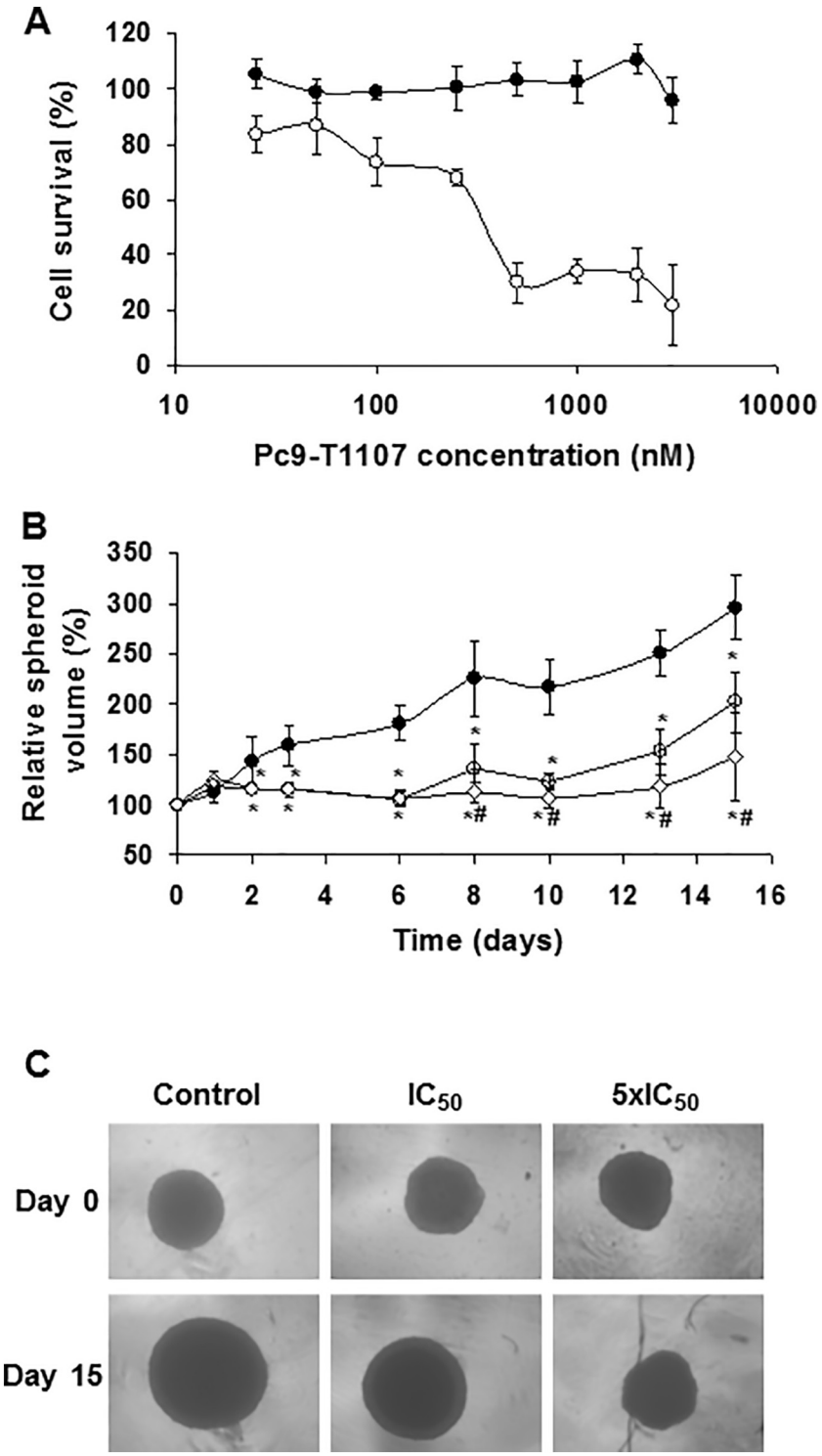

Fig. 7. Pc9-T1107-induced cytotoxic effect on CT26 spheroids. (A) Different concentrations of Pc9-T1107 were incubated with CT26 spheroids in the dark (●) or exposed to a light dose of 2.8 J cm^{-2} (○). MTT assay was performed 24 h after treatment. (B) Growth kinetics of spheroids incubated in the absence (●) or presence of IC_{50} (○) or 5 × IC_{50} of Pc9-T1107 (◊). Results represent the mean ± S.E.M., n = 3, $^{*}p < 0.05$, significantly different from spheroids incubated in the absence of phthalocyanine, $^{\#}p < 0.05$, significantly different from spheroids incubated with IC_{50} of Pc9-T1107. (C) Phase contrast images of CT26 spheroids incubated in the absence or presence of different concentrations of phthalocyanine before irradiation or 15 days after treatment. Magnification: 40 ×.

well as in 3D cultures suggested the involvement of the executioner caspase-3, a cysteine protease that cleaves a variety of cellular substrates responsible for the typical changes that occur during apoptosis [55–58]. This first evidence of an apoptotic death was then confirmed by the increase in the proteolytic activity of this protease, although further experiments will be required to assess the involvement of the cell death receptor pathway and/or the mitochondrial pathway. Other authors, using polymeric micelles-based photosensitizers, including phthalocyanines and Photofrin, have also reported the induction of photodamage through the activation of an apoptotic type of cell death [24,25]. Despite these findings, the contribution of other cell death programs, such as necrosis or autophagy, in the photocytoxic action triggered by Pc9 in colon cancer cells cannot yet be discarded.

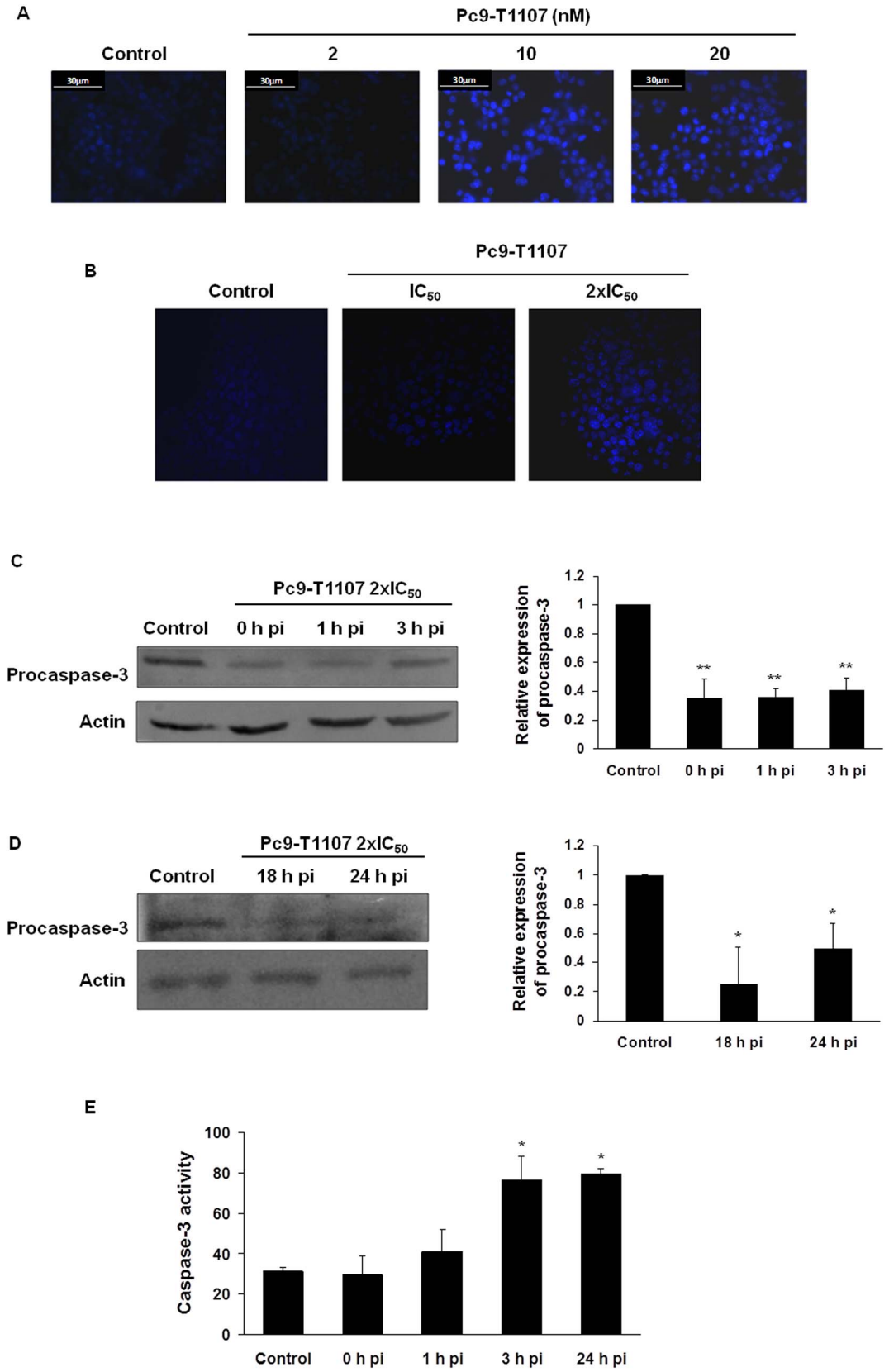

Fig. 8. Induction of an apoptotic response after PDT. CT26 cells incubated with different concentrations of Pc9-T1107 were stained immediately after irradiation (A) or 24 h post-irradiation (B) with Höechst 33258. Control corresponds to non-irradiated cells. Cell nuclei from 2D (A) and 3D (B) cultures were visualized with a confocal microscope. Magnification: 400 × (A), 600 × (B). (C) CT26 cells exposed to 2 × IC_{50} of Pc9-T1107 were irradiated (0 h p.i.), incubated for 1 or 3 h and submitted to Western blot assays. Non-treated cells were used as control. (D) Western blot analysis of procaspase-3 from CT26 spheroids exposed to 2 × IC_{50} of Pc9-T1107 and incubated 18 h or 24 h post-irradiation. Densitometric analyses, expressed as the relationship of procaspase-3 from Pc9-treated cells (C) or Pc9-treated CT26 spheroids (D) with respect to non-treated cells, correspond to mean ± S.E.M. of three different experiments. *$p < 0.05$; **$p < 0.005$, significantly different from control. (E) After incubation of 2D CT26 cultures for 24 h with 2 × IC_{50} of Pc9-T1107, cells were irradiated, lysed and caspase-3 activity was measured at different times by using a fluorometer.

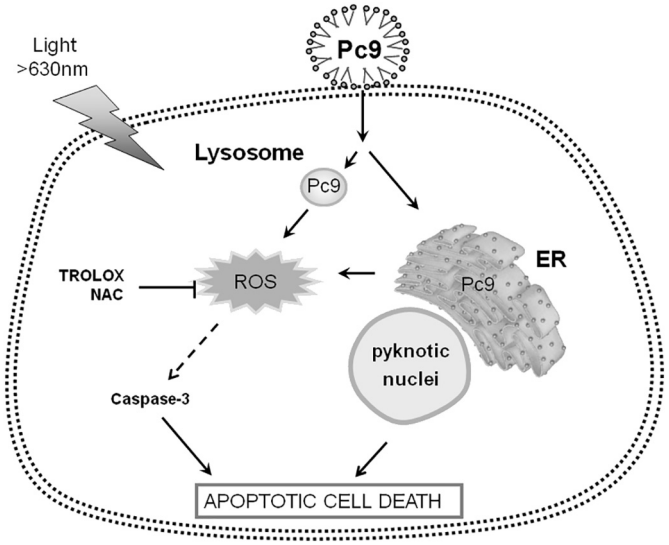

Fig. 9. Proposed model of Pc9-induced cell death in CT26 cells. The formation of ROS after irradiation in the primary sites of Pc9 accumulation leads to the cleavage of the procaspase-3 and the detection of pyknotic nuclei, suggesting the induction of an apoptotic response.

5. Conclusion

In summary, we demonstrated that the lipophilic Pc9 phthalocyanine encapsulated into T1107 poloxamine micelles is internalized and mainly accumulated in lysosomes and endoplasmic reticulum. These organelles represent the primary sites of ROS formation, the cytotoxic species that initiate the series of events contributing to cell death (Fig. 9). The effectiveness of this formulation as a photocytotoxic agent that induces an apoptotic cell death was demonstrated in 2D as well as in 3D culture models. Since spheroids models are a good option to approach closer to the structure of the tumor developed *in vivo*, these findings encourage us to evaluate the effect of Pc9-T1107 in a murine colon carcinoma model.

Acknowledgments

This work was supported by grants from Consejo Nacional de Investigaciones Científicas y Técnicas (CONICET, PIP 066: “Estudio de los mecanismos de acción de citoquinas y flavonoides que regulan el crecimiento celular”), Universidad de Buenos Aires (Programación Científica 2014–2017, UBACYT 20020130100024: “Mecanismos de acción de moléculas que intervienen en procesos que regulan la proliferación celular: rol de citoquinas y nuevos agentes antitumorales”), and Agencia Nacional de Promoción Científica y Tecnológica (PICT-2013-0144: “Propiedades fotodinámicas de ftalocianinas de Zinc (II) en un modelo de carcinoma de colon *in vivo*”).

References

[1] F.A. Haggar, R.P. Boushey, Colorectal cancer epidemiology: incidence, mortality, survival, and risk factors, Clin. Colon Rectal Surg. 22 (2009) 191–197.
[2] F.T. Kolligs, Diagnostics and epidemiology of colorectal cancer, Visc. Med. 32 (2016) 158–164.
[3] P. Favoriti, G. Carbone, M. Greco, F. Pirozzi, R.E. Pirozzi, F. Corcione, Worldwide burden of colorectal cancer: a review, Updat. Surg. 68 (2016) 7–11.
[4] B. Doleman, K.T. Mills, S. Lim, M.D. Zelhart, G. Gagliardi, Body mass index and colorectal cancer prognosis: a systematic review and meta-analysis, Tech. Coloproctol. 20 (2016) 517–535.
[5] V. Aran, A.P. Victorino, L.C. Thuler, C.G. Ferreira, Colorectal cancer: epidemiology, disease mechanisms and interventions to reduce onset and mortality, Clin. Colorectal Cancer 15 (2016) 195–203.
[6] E.A. Platz, W.C. Willett, G.A. Colditz, E.B. Rimm, D. Spiegelman, E. Giovannucci, Proportion of colon cancer risk that might be preventable in a cohort of middle-aged US men, Cancer Causes Control 11 (2000) 579–588.
[7] H. Patil, S.G. Saxena, C.J. Barrow, J.R. Kanwar, A. Kapat, R.K. Kanwar, Chasing the personalized medicine dream through biomarker validation in colorectal cancer, Drug Discov. Today 22 (2017) 11–119.
[8] T.J. Dougherty, C.J. Gomer, B.W. Henderson, G. Jori, D. Kessel, M. Korbelik, J. Moan, Q. Peng, Photodynamic therapy, J. Natl. Cancer Inst. 90 (1998) 889–905.
[9] S.M. Fien, A.M. Oseroff, Photodynamic therapy for non-melanoma skin cancer, J. Natl. Compr. Cancer Netw. 5 (2007) 531–540.
[10] R. Josefsen, W. Boyle, Photodynamic therapy: novel third-generation photosensitizers one step closer? Br. J. Pharmacol. 154 (2008) 1–3.
[11] M.G.H. Vicente, Porphyrin-based sensitizers in the detection and treatment of cancer: recent progress, Curr. Med. Chem. Anticancer Agents 1 (2001) 175–194.
[12] M.R. Detty, S.L. Gibson, S.J. Wagner, Current clinical and preclinical photosensitizers for use in photodynamic therapy, J. Med. Chem. 47 (2004) 3897–3915.
[13] H. Kato, Photodynamic therapy for lung cancer—a review of 19 years' experience, J. Photochem. Photobiol. B 42 (1998) 96–99.
[14] A. Maier, U. Anegg, B. Fell, P. Rehak, B. Ratzenhofer, F. Tomaselli, O. Sankin, H. Pinter, F.M. Smolle-Jüttner, G.B. Friehs, Hyperbaric oxygen and photodynamic therapy in the treatment of advanced carcinoma of cardia and esophagus, Lasers Surg. Med. 26 (2000) 308–315.
[15] R.M. Szeimies, C.A. Morton, A. Sidoroff, L.R. Braathen, Photodynamic therapy for nonmelanoma skin cancer, Acta Derm. Venereol. 85 (2005) 483–490.
[16] C. Fabris, G. Valduga, G. Miotto, L. Borsetto, G. Jori, S. Garbisa, E. Reddi, Photosensitization with zinc (II) phthalocyanine as a switch in the decision between apoptosis and necrosis, Cancer Res. 15 (2001) 7495–7500.
[17] J. Marino, M.C. Garcia Vior, L.E. Dicelio, L.P. Roguin, J. Awruch, Photodynamic effects of isosteric water-soluble phthalocyanines on human nasopharynx KB carcinoma cells, Eur. J. Med. Chem. 45 (2010) 4129–4139.
[18] P. Margaron, M.J. Grégoire, V. Scasnárt, H. Ali, J.E. van Lier, Structure-photodynamic activity relationships of a series of 4-substituted zinc phthalocyanines, Photochem. Photobiol. 63 (1996) 217–223.
[19] V.C. Colussi, D.K. Feyes, J.W. Mulvihill, Y.S. Li, M.E. Kenney, C.A. Elmets, N.L. Oleinick, H. Mukhtar, Phthalocyanine 4 (Pc 4) photodynamic therapy of human OVCAR-3 tumor xenografts, Photochem. Photobiol. 69 (1999) 236–241.
[20] J.P. Taquet, C. Frochot, V. Manneville, M. Barberi-Heyob, Phthalocyanines covantely bound to biomolecules for a targeted photodynamic therapy, Curr. Med. Chem. 14 (2007) 1673–1687.
[21] V.P. Torchilin, Multifunctional nanocarriers, Adv. Drug Deliv. Rev. 58 (2006) 1532–1555.
[22] M.C. García Vior, E. Monteagudo, L.E. Dicelio, J. Awruch, A comparative study of a novel lipophilic phthalocyanine incorporated into nanoemulsion formulations: photophysics, size, solubility and thermodynamic stability, Dyes Pigments 91 (2011) 208–214.
[23] D.A. Chiappetta, A. Sosnik, Poly(ethylene oxide)-poly (propylene oxide) block copolymer micelles as drug delivery agents: improved hydrosolubility, stability and bioavailability of drugs, Eur. J. Pharm. Biopharm. 66 (2007) 303–317.
[24] L. Lamch, J. Kulbacka, J. Pietkiewicz, J. Rossowska, M. Dubińska-Magiera, A. Choromańska, K.A. Wilk, Preparation and characterization of new zinc(II) phthalocyanine—containing poly(L-lactide)-b-poly(ethylene glycol) copolymer micelles for photodynamic therapy, J. Photochem. Photobiol. B Biol. 160 (2016) 185–197.
[25] L. Lamch, U. Bazylinska, J. Kulbacka, J. Pietkiewicz, K. Biezunska-Kusiak, K.A. Wilk, Polymeric micelles for enhanced PhotofrinII® delivery, cytotoxicity and pro-apoptotic activity in human breast and ovarian cancer cells, Photodiagn. Photodyn. Ther. 11 (2014) 570–585.
[26] L. Lamch, W. Tylus, M. Jewginski, R. Latajka, K.A. Wilk, Location of varying hydrophobicity zinc (II) phthalocyanine-type photosensitizers in methoxy poly (ethylene oxide) and poly(L-lactide) block copolymer micelles using H NMR and XPS techniques, J. Phys. Chem. B 120 (2016) 12768–12780.
[27] N.C. López Zeballos, J. Marino, M.C. García Vior, N. Chiarante, L.P. Roguin, J. Awruch, L.E. Dicelio, Photophysics and photobiology of different liposomal formulations of 2,9(10),16(17),23(24)-tetrakis[(2dimethylamino)ethylsulfanyl] phthalocyaninato-zinc(II), Dyes Pigments 96 (2013) 626–635.
[28] M.C. García Vior, J. Marino, L.P. Roguin, A. Sosnik, J. Awruch, Photodynamic effects of zinc(II) phthalocyanine-loaded polymeric micelles in human nasopharynx KB carcinoma cells, Photochem. Photobiol. 89 (2013) 492–500.
[29] J. Marino, M.C. García Vior, V.A. Furmento, V.C. Blank, J. Awruch, L.P. Roguin, Lysosomal and mitochondrial permeabilization mediates zinc(II) cationic phthalocyanine phototoxicity, Int. J. Biochem. Cell Biol. 45 (2013) 2553–2562.
[30] J. Friedrich, C. Siedel, R. Ebner, L.A. Kunz-Schughart, Spheroid-based drug screen: considerations and practical approach, Nat. Protoc. 4 (2009) 309–324.
[31] G. Mehta, A.Y. Hsiao, M.I. Ingram, G.D. Luker, S. Takayama, Opportunities and challenges for use of tumor spheroids as models to test drug delivery and efficacy, J. Control. Release 164 (2012) 192–204.
[32] J.M. Dąbrowski, L.G. Arnaut, Photodynamic therapy (PDT) of cancer: from local to systemic treatment, Photochem. Photobiol. Sci. 14 (2015) 1765–1780.
[33] A. Kawczyk-Krupka, A.M. Bugaj, W. Latos, K. Zaremba, K. Wawrzyniec, A. Sieroń, Photodynamic therapy in colorectal cancer treatment: the state of the art in clinical trials, Photodiagn. Photodyn. Ther. 12 (2015) 545–553.
[34] T. Hatakeyama, Y. Murayama, S. Komatsu, A. Shiozaki, Y. Kuriu, H. Ikoma, M. Nakanishi, D. Ichikawa, H. Fujiwara, K. Okamoto, T. Ochiai, Y. Kokuba, K. Inoue, M. Nakajima, E. Otsuji, Efficacy of 5-aminolevulinic acid-mediated photodynamic therapy using light-emitting diodes in human colon cancer cells, Oncol. Rep. 29 (2013) 911–916.
[35] T. Namikawa, T. Yatabe, K. Inoue, T. Shuin, K. Hanazaki, Clinical applications of 5-aminolevulinic acid-mediated fluorescence for gastric cancer, World J. Gastroenterol. 21 (2015) 8769–8775.
[36] P.G. Calzavara-Pinton, M. Venturini, R. Sala, Photodynamic therapy: update 2006.

Part 1: photochemistry and photobiology, J. Eur. Acad. Dermatol. Venereol. 21 (2007) 293–302.
[37] J.D. Miller, E.D. Baron, H. Scull, A. Hsia, J.C. Berlin, T. McCormick, V. Colussi, M.E. Kenney, K.D. Cooper, N.L. Oleinick, Photodynamic therapy with the phthalocyanine photosensitizer Pc 4: the case experience with preclinical mechanistic and early clinical-translational studies, Toxicol. Appl. Pharmacol. 224 (2007) 290–299.
[38] R.R. Allison, C.H. Sibata, Oncologic photodynamic therapy photosensitizers: a clinical review, Photodiagn. Photodyn. Ther. 7 (2010) 61–75.
[39] A. Kawczyk-Krupka, A.M. Bugaj, W. Latos, K. Zaremba, K. Wawrzyniec, M. Kucharzewski, A. Sieroń, Photodynamic therapy in colorectal cancer treatment—the state of the art in preclinical research, Photodiagn. Photodyn. Ther. 13 (2016) 158–174.
[40] U. Kedar, P. Phutane, S. Shidhaye, V. Kadam, Advances in polymeric micelles for drug delivery and tumor targeting, Nanomedicine 6 (2010) 714–729.
[41] R.G. Strickley, Solubilizing excipients in oral and injectable formulations, Pharm. Res. 21 (2004) 201–230.
[42] J. Friedrich, R. Ebner, L.A. Kunz-Schughart, Experimental anti-tumor therapy in 3-D: spheroids—old hat or new challenge? Int. J. Radiat. Biol. 83 (2007) 849–871.
[43] R.Z. Lin, H.Y. Chang, Recent advances in three-dimensional multicellular spheroid culture for biomedical research, Biotechnol. J. 3 (2008) 1172–1184.
[44] Y.S. Torisawa, A. Takagi, H. Shiku, T. Yasukawa, T. Matsue, A multicellular spheroid-based drug sensitivity test by scanning electrochemical microscopy, Oncol. Rep. 13 (2005) 1107–1112.
[45] Y. Imamura, T. Mukohara, Y. Shimono, Y. Funakoshi, N. Chayahara, M. Toyoda, N. Kiyota, S. Takao, S. Kono, T. Nakatsura, H. Minami, Comparison of 2D- and 3D-culture models as drug-testing platforms in breast cancer, Oncol. Rep. 33 (2015) 1837–1843.
[46] P. Agostinis, K. Berg, K.A. Cengel, T.H. Foster, A.W. Girotti, S.O. Gollnick, S.M. Hahn, M.R. Hamblin, A. Juzeniene, D. Kessel, M. Korbelik, J. Moan, P. Mroz, D. Nowis, J. Piette, B.C. Wilson, J. Golab, Photodynamic therapy of cancer: an update, CA Cancer J. Clin. 61 (2011) 250–281.
[47] B.W. Henderson, T.J. Dougherty, How does photodynamic therapy work? Photochem. Photobiol. 55 (1992) 145–157.
[48] W.M. Sharman, C.M. Allen, J.E. van Lier, Photodynamic therapeutics: basic principles and clinical applications, Drug Discov. Today 11 (1999) 507–517.
[49] R.R. Allison, V.S. Bagnato, C.H. Sibata, Future of oncologic photodynamic therapy, Future Oncol. 6 (2010) 929–940.
[50] N.L. Oleinick, R.L. Morris, I. Belichenko, The role of apoptosis in response to photodynamic therapy: what, where, why, and how, Photochem. Photobiol. Sci. 1 (2002) 1–21.
[51] S.M. Chiu, L.Y. Xue, M. Lam, M.E. Rodriguez, P. Zhang, M.E. Kenney, A.L. Nieminen, N.L. Oleinick, A requirement for bid for induction of apoptosis by photodynamic therapy with a lysosome—but not a mitochondrion-targeted photosensitizer, Photochem. Photobiol. 86 (2010) 1161–1173.
[52] R.C. Krieg, H. Messmann, K. Schlottmann, E. Endlicher, S. Seeger, J. Schölmerich, R. Knuechel, Intracellular localization is a cofactor for the phototoxicity of protoporphyrin IX in the gastrointestinal tract: in vitro study, Photochem. Photobiol. 78 (2003) 393–399.
[53] S. Marchal, A. Fadloun, E. Maugain, M.A. D'Hallewin, F. Guillemin, L. Bezdetnaya, Necrotic and apoptotic features of cell death in response to Foscan photosensitization of HT29 monolayer and multicell spheroids, Biochem. Pharmacol. 69 (2005) 1167–1176.
[54] M.B. Gariboldi, R. Ravizza, P. Baranyai, E. Caruso, S. Banfi, S. Meschini, E. Monti, Photodynamic effects of novel 5,15-diaryl-tetrapyrrole derivatives on human colon carcinoma cells, Bioorg. Med. Chem. 17 (2009) 2009–2016.
[55] M.O. Hengartner, The biochemistry of apoptosis, Nature 407 (2000) 770–776.
[56] M.G. Grutter, Caspases: key players in programmed cell death, Curr. Opin. Struct. Biol. 10 (2000) 649–655.
[57] S.H. Kaufmann, M.O. Hengartner, Programmed cell death: alive and well in the new millennium, Trends Cell Biol. 11 (2001) 526–534.
[58] N.N. Danial, S.J. Korsmeyer, Cell death: critical control points, Cell 116 (2004) 205–219.